

# EXCLUSIVE PRODUCTION OF $\eta$ MESON IN PROTON–PROTON COLLISIONS AT FAIR ENERGIES\*

PIOTR LEBIEDOWICZ 

Institute of Nuclear Physics Polish Academy of Sciences  
Radzikowskiego 152, 31-342 Kraków, Poland

*Received 25 March 2025, accepted 27 March 2025,  
published online 12 May 2025*

We discuss the exclusive production of  $\eta$  meson in proton–proton collisions in order to learn about the relevant production mechanism at the GSI-FAIR energies. The nucleon and baryonic-resonance amplitudes are derived within an effective Lagrangian approach. Assuming that for the  $pp \rightarrow pp\eta$  reaction the dominant contribution is due to an excitation of  $N(1535)$  via the  $\rho^0$  exchange, the present model reproduces data for both total and differential cross sections, for instance, the distributions of the polar angle of the  $\eta$  meson in the center-of-mass system. The role of vector-meson-fusion processes  $\omega\omega, \rho^0\rho^0 \rightarrow \eta$  is specified. Comparisons with currently existing data from the DISTO and HADES experiments are made, and predictions for higher energies (HADES, PANDA, SIS100) are given.

DOI:10.5506/APhysPolBSupp.18.4-A7

## 1. Introduction

The reaction  $pp \rightarrow pp\eta$  was addressed in several experimental works, *e.g.*, [1–4] and in theoretical works, but mainly at the energies close to the reaction threshold; see *e.g.* [5–8]. In this presentation, we concentrate on the production mechanism at higher energies where the existing data are rather scarce. Nevertheless, there are efforts to improve or extend cross-section database, in particular at the GSI facilities in Darmstadt (Germany). In February 2022, proton–proton reactions at 4.5 GeV beam kinetic energy (center-of-mass energy  $\sqrt{s} = 3.46$  GeV) were measured by the HADES Collaboration [9]. It will therefore provide valuable experimental results to test our predictions for the exclusive production of the  $\eta$  meson and other resonances<sup>1</sup>. Additional experiments in the intermediate energy range (PANDA,

\* Presented at the Workshop at 1 GeV scale: From mesons to axions, Kraków, Poland, 19–20 September, 2024.

<sup>1</sup> In [10], the exclusive production of the  $f_1(1285)$  meson in the context of future measurements with the HADES and PANDA detectors at GSI-FAIR was discussed.

SIS100) would be greatly appreciated. We shall learn from the  $\eta$  production at GSI about the  $\eta NN$ ,  $\eta NN^*$ ,  $\rho NN^*$  coupling strengths, in particular those involving the  $N(1535)$  resonance which has a large branching ratio into  $N\eta$  of 30–55% and  $N\rho$  of 2–17% [12]. At higher energies, the central exclusive production of  $\eta$  and  $\eta'$  mesons in  $pp$  collisions was discussed in [11] within the tensor–Pomeron approach. Such measurements would facilitate further insight into the nature of the  $\eta$  and  $\eta'$  mesons, in particular the characteristics of their production mechanism.

## 2. Sketch of the formalism

We study the exclusive reaction

$$p(p_a) + p(p_b) \rightarrow p(p_1) + p(p_2) + \eta(k), \quad (1)$$

where  $p_{a,b}$ ,  $p_{1,2}$  denote the four-momenta of the protons and  $k$  denotes the four-momentum of the  $\eta$  meson. The cross section is as follows:

$$\sigma = \frac{1}{2} \frac{1}{2\sqrt{s(s-4m_p^2)}} \int \frac{d^3k}{(2\pi)^3 2k^0} \frac{d^3p_1}{(2\pi)^3 2p_1^0} \frac{d^3p_2}{(2\pi)^3 2p_2^0} \times (2\pi)^4 \delta^{(4)}(p_1 + p_2 + k - p_a - p_b) \frac{1}{4} \sum_{\text{spins}} |\mathcal{M}_{pp \rightarrow pp\eta}|^2, \quad (2)$$

where  $\mathcal{M}_{pp \rightarrow pp\eta} = \mathcal{M}_{pp \rightarrow pp\eta}(p_1, p_2) - \mathcal{M}_{pp \rightarrow pp\eta}(p_2, p_1)$ . The full amplitude includes the basic  $\eta$ -production mechanisms shown in Fig. 1. There,  $N$  and  $N^*$  denote the intermediate proton and resonance  $N(1535)$ , respectively, and  $M$  incorporates an exchange of meson (*e.g.*,  $\pi^0$ ,  $\rho^0$ )<sup>2</sup>. To evaluate

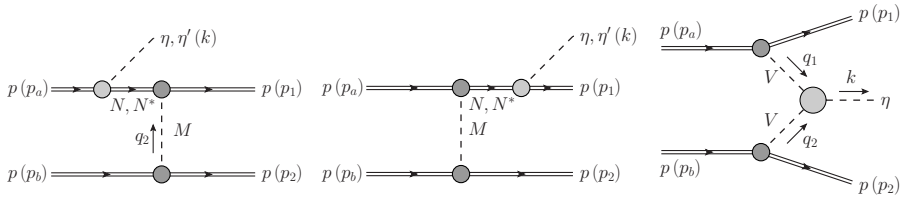


Fig. 1. Feynman diagrams contributing to  $pp \rightarrow pp\eta$ . The diagrams on the left show the processes via intermediate nucleon or nucleon resonances. There are also the corresponding diagrams with the  $\eta$  emission from the lower proton lines. The diagram on the right represents the  $VV$ -fusion mechanism where  $VV$  stands for  $\omega\omega$  or  $\rho^0\rho^0$ .

<sup>2</sup> The  $\rho$ -exchange contribution is clearly favored when comparing the model with the DISTO data; see Fig. 3. The angular distributions should be forward peaked if  $\pi^0$  exchange would be dominant.

the amplitude, one needs to know the propagators for various baryons and mesons as well as the vertices involving the phenomenological form-factor functions. To illustrate, in the case of  $\eta$  production which proceeds via the excitation of the  $N(1535)$  ( $J^P = 1/2^-$ ) resonance through the  $\rho$  exchange, the effective Lagrangian for the coupling  $\rho NN(1535)$  can be written as [8]

$$\mathcal{L}_{\rho NN^*} = -\frac{1}{2m_N} \bar{N}^* \gamma_5 \left[ g \left( \frac{\gamma_\mu \partial^2}{m_{N^*} + m_N} - i \partial_\mu \right) - f \sigma_{\mu\nu} \partial^\nu \right] (\tau \Phi_\rho^\mu) N + \text{h.c.} \quad (3)$$

There is the vector (PV)- and tensor (PT)-type coupling with the corresponding coupling constants  $g$  and  $f$ , respectively, and they are treated as free parameters to be determined by fitting to the data. In principle, one can select a linear combination of both and fit the  $g/f$  ratio to the data. However, to minimize the number of parameters, we choose either PV- or PT-type coupling at a time. In these calculations, the vertex  $\Gamma_\mu^{(\rho NN^*)}$  derived from (3) is supplemented by the form factor

$$F_{\rho NN^*}(q^2, p_N^2, p_{N^*}^2) = F_\rho(q^2) F_B(p_N^2) F_B(p_{N^*}^2), \\ F_\rho(q^2) = \frac{\Lambda_\rho^2 - m_\rho^2}{\Lambda_\rho^2 - q^2}, \quad F_B(p^2) = \frac{\Lambda_B^4}{(p^2 - m_B^2)^2 + \Lambda_B^4}, \quad B = N, N^*, \quad (4)$$

where  $q^2$  and  $p^2$  denote the four-momenta squared of off-shell meson and baryon, respectively. We take the cut-off parameters  $\Lambda_\rho = 1.4$  GeV,  $\Lambda_N = 1.0$  GeV,  $\Lambda_{N^*} = 1.2$  GeV.

The main features of the  $VV$ -fusion mechanism are known from (2.4) of [10] but with the replacement:  $\Gamma_{\nu_1 \nu_2 \alpha}^{(VV f_1)}(q_1, q_2)(\epsilon^\alpha)^* \rightarrow \Gamma_{\nu_1 \nu_2}^{(VV \eta)}(q_1, q_2)$ . In order to determine some of the model parameters, the  $\pi^- p \rightarrow \eta n$  and  $\gamma p \rightarrow \eta p$  reactions were considered and results were compared with the available data for cross sections for these reactions.

### 3. Preliminary results for the $pp \rightarrow pp\eta$ reaction

Our theoretical results are shown in Figs. 2 and 3 together with the experimental data. Figure 2 shows that our calculation with the  $N(1535)$ -resonance domination reproduces energy dependence of the measured cross sections. For the  $N$  and  $N(1535)$  contributions via the  $\rho^0$ -meson exchange, the relevant amplitudes were multiplied by a suppression function:  $f(s) = \exp\left(-\frac{s-s_{\text{thr}}}{\Lambda^2}\right)$  with  $s_{\text{thr}} = (2m_p + m_\eta)^2$  and  $\Lambda = 4$  GeV. We see that the  $N(1535)$  contribution is the dominant production mechanism, although the nucleonic ( $N$ ) and mesonic ( $VV$  fusion) contributions become important,

especially when energy increases. It should be noted that an interference of various contributions is not negligible there. For  $\sqrt{s} = 3.46$  GeV (HADES), we predict  $\sigma \simeq 116 \mu\text{b}$ , for  $\sqrt{s} = 8$  GeV (SIS100), we predict  $\sigma \simeq 5 \mu\text{b}$ <sup>3</sup>.

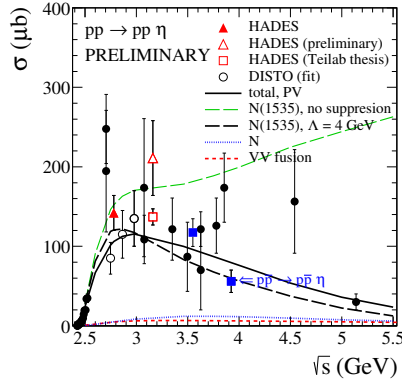


Fig. 2. Total cross section for the  $pp \rightarrow pp\eta$  reaction as a function of collision energy  $\sqrt{s}$ . Shown are the model results together with the experimental data from [1–4] and from low-statistics bubble-chamber experiments. The model results for complete (total) and individual contributions for the  $N(1535)$ ,  $N$ , and  $VV$ -fusion mechanisms are shown.

From Fig. 3, we can see that by adjusting the  $\rho NN(1535)$  coupling constant in (3), the model gives a reasonable description of the DISTO data [1]. Here, two options are exercised: (PV) pure vector coupling with  $g_{\rho NN^*} = -8.0$ , (PT) pure tensor coupling with  $f_{\rho NN^*} = 4.0$ . The total cross sections calculated for these options differ only slightly. For a better understanding of the dynamics of the  $pp \rightarrow pp\eta$  reaction, more experimental data at higher energies and differential distributions are desirable. Hopefully, the HADES measurement at  $\sqrt{s} = 3.46$  GeV, discussed *e.g.* in [9], will provide valuable information.

#### 4. Summary

In this contribution, we highlighted the recent progress made towards achieving description of experimental data measured by the DISTO and HADES collaborations for the  $pp \rightarrow pp\eta$  reaction, significantly further from the reaction threshold, within a simplified model based on an effective Lagrangian approach. The calculated cross sections are based on a model that takes into account the interference effects between the processes considered. It would appear that the dominant mechanism in this reaction, further from the threshold (at DISTO and HADES energies) proceeds via the excitation

<sup>3</sup> For further results, we refer to <https://indico.meson.if.uj.edu.pl/event/5/>

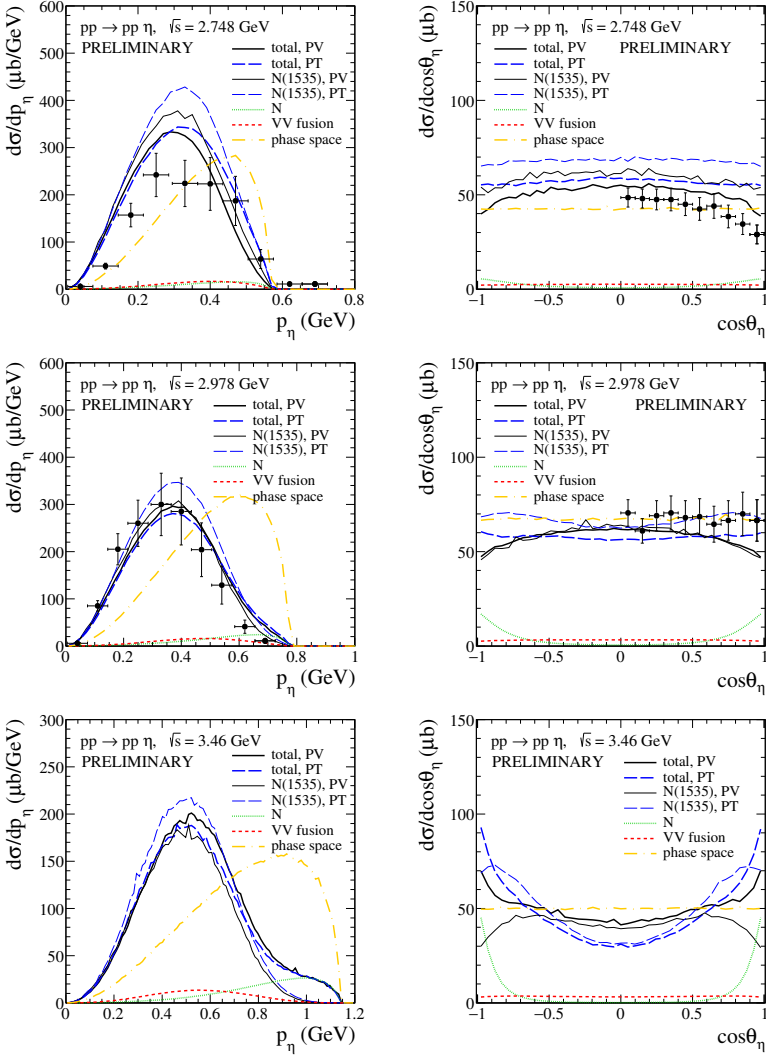


Fig. 3. Differential cross sections *versus* the c.m. momentum of the  $\eta$  meson (left) and  $\cos\theta_\eta$  (right). The model results are compared with the DISTO data from [1]. The solid and long-dashed thick lines correspond to the complete model which includes  $N(1535)$ ,  $N$ , and  $VV$ -fusion contributions, whereas the thin lines reflect the results for the PV- and PT-type coupling for the  $\rho NN(1535)$  vertex. Individual contributions from the  $N$  and  $VV$ -fusion processes are also shown. The long-dash-dotted lines correspond to the results for pure phase space (presented for comparison purposes only) normalised to the DISTO data, but in the case of  $\sqrt{s} = 3.46$  GeV to  $100 \mu\text{b}$ .

of the  $N(1535)$  intermediate resonance via the  $\rho$  exchange, while the nucleonic and reggeized-vector-meson-fusion processes are expected to be more relevant at higher energies (PANDA, SIS100). In the  $\rho NN(1535)$  vertex, derived from (3), we have assumed that only the vectorial (PV) or tensorial (PT) term is involved. We obtain a good description of the DISTO data [1] for the polar angle and momentum distributions of the  $\eta$  at proton–proton collision energies  $\sqrt{s} = 2.748\text{--}2.978$  GeV. We have made first predictions for the HADES experiment for  $\sqrt{s} = 3.46$  GeV. The results for the  $pp \rightarrow pp\eta'$  reaction have been calculated as well, but are not presented in this article. There, the role of  $VV$ -fusion processes is even more important.

Studies of exclusive  $\eta$  production present interesting challenges from a theoretical perspective and are phenomenologically relevant for completed (DISTO, HADES) and upcoming (PANDA, SIS100 [13]) experiments at GSI-FAIR. To learn more information about the  $pp \rightarrow pp\eta$  reaction mechanism, in particular to constrain the coupling strengths involving the  $N(1535)$  resonance, the experimental study of cross section over a broad energy range as well as of the angular distributions seems to be crucial.

I would like to thank the organisers of this workshop for making this presentation of first results possible. Useful discussions with I. Ciepał, P. Salabura, A. Szczurek, S. Trelinski, and M. Zieliński are gratefully acknowledged.

## REFERENCES

- [1] DISTO Collaboration (F. Balestra *et al.*), *Phys. Rev. C* **69**, 064003 (2004).
- [2] HADES Collaboration (K. Teilab), *Int. J. Mod. Phys. A* **26**, 694 (2011).
- [3] K. Teilab, Ph.D. Thesis, «The production of  $\eta$  and  $\omega$  mesons in 3.5 GeV  $p+p$  interaction in HADES», Frankfurt U., 2011, <https://hades.gsi.de/node/4>
- [4] HADES Collaboration (G. Agakishiev *et al.*), *Eur. Phys. J. A* **48**, 74 (2012).
- [5] G. Fäldt, C. Wilkin, *Phys. Scr.* **64**, 427 (2001).
- [6] L.P. Kaptari, B. Kämpfer, *Eur. Phys. J. A* **33**, 157 (2007).
- [7] R. Shyam, *Phys. Rev. C* **75**, 055201 (2007).
- [8] K. Nakayama, Y. Oh, H. Haberzettl, *J. Korean Phys. Soc.* **59**, 224 (2011).
- [9] S. Trelinski, *Acta Phys. Pol. B Proc. Suppl.* **18**, XXX (2025), this issue.
- [10] P. Lebedowicz, O. Nachtmann, P. Salabura, A. Szczurek, *Phys. Rev. D* **104**, 034031 (2021).
- [11] P. Lebedowicz, O. Nachtmann, A. Szczurek, *Ann. Phys.* **344**, 301 (2014).
- [12] Particle Data Group (S. Navas *et al.*), *Phys. Rev. D* **110**, 030001 (2024).
- [13] QCD at FAIR Workshop 2024, <https://indico.gsi.de/event/20301/>